Damage-Resistant Brittle Coatings

By *Brian R. Lawn*,* *Kee Sung Lee*, *Herzl Chai*, *Antonia Pajares*, *Do Kyung Kim*, *Sataporn Wuttiphan*, *Irene M. Peterson*, and *Xiaozhi Hu*

Laminate structures consisting of hard, brittle coatings and soft, tough substrates are important in a wide variety of engineering applications (cutting tools, electronic multilayers, laminated windscreens), biological structures (teeth and dental crowns, shells, bones), and traditional pottery (ceramic glazes). A hard outerlayer variously offers increased load-bearing capacity, wear resistance, thermal and corrosion protection, electrical insulation, and aesthetics; a compliant underlayer offers stress redistribution and damage tolerance. But hard layers are susceptible to cracking, especially in surface-concentrated loads from static or cyclic contacts. In natural or restorative tooth structures, for instance, forces in excess of 100 N operate at contacts between opposing cusps of characteristic radii 2–4 mm over 10^7 cycles, leading to occasional premature failures.[1] The stress field in the supported brittle coating is Hertzian-like in the near-contact region and flexure-like in the far-contact region, with resultant competing modes of fracture and damage, including some new modes not observed in monolithic materials. These damage modes determine the useful lifetime of the layer structure.

Conventional design of brittle layer structures is based on a philosophy of "crack containment", i.e., preventing already well-developed cracks in the coating from penetrating into adjacent layers, so increasing the effective "toughness" of the composite structure. Several approaches of this kind have been proposed:[2] i) Crack deflection along weak interfaces between hard layers. Cracks are deflected out of the main tensile field along weak orthogonal interlayer interfaces.[3,4] ii) Crack inhibition from intralayer residual compression. Thermal expansion mismatch introduces compression stresses into one or other of the layers during fabrication, inhibiting crack extension,[5] with possible lower-limit thresholds for interlayer crack penetration.[6] iii) Crack arrest in tough substrates. Cracks enter a toughened sublayer where they are slowed and arrested.[7–9] iv) Crack confinement by stress redistribution. Incorporation of a soft underlayer with a strong interface redirects and confines cracks within the boundaries of the outer coating.[10–12] Generally, effective crack containment calls for thinner brittle layers and higher interlayer mismatch.

Crack-containment approaches are viable where limited cracking in brittle outerlayers is tolerable (e.g., automobile windshields, thermal shock applications). But in many applications one cannot sustain even a single crack (e.g., dental crowns, ceramic-coated cutting tools, corrosion protective coatings, electronic multilayer devices). Such cracks may occur at much lower loads than those needed to cause ultimate failure. The problem is exacerbated in prolonged or cyclic loading, where even the smallest of cracks or other inelastic damage can evolve steadily but inexorably into a catastrophic failure.[13,14] A more conservative approach is called for—one must design against crack initiation rather than crack propagation. The idea is not so much to contain cracks once they start, but to prevent them from starting in the first place. This can lead to conflicting requirements in layer dimensions and material properties.

In this study we introduce a new approach to the design of damage-resistant brittle coatings, based on a combination of new and existing relations for crack initiation in well-defined contact-induced stress fields. Consider a brittle layer of thickness d on a compliant substrate, with a well-bonded interface, subjected to contact at load P with a sphere of radius r, Figure 1. The coating is considered to be thin enough that it flexes under the applied contact. Since we are interested in first damage in the brittle coating, we may treat the system as elastic up to the critical load. There are two main fracture modes,[15] both of which initiate from some surface flaw:

Cone cracks: This kind of fracture is well documented from decades of research on monolithic brittle solids. The crack first develops from the top surface outside the contact circle, where the tensile stress is maximum, as a shallow, stable surface ring within a rapidly diminishing subsurface tensile field; it then pops in to its ultimate (truncated) cone-like geometry at a critical load

[*] *Prof. B. R. Lawn, Dr. K. S. Lee*
Materials Science and Engineering Laboratory
National Institute of Standards and Technology
Gaithersburg, MD 20899 (USA)
Dr. H. Chai
Department of Solid Mechanics, Materials and Structures
Faculty of Engineering, Tel Aviv University
Tel Aviv 69978 (Israel)
Dr. A. Pajares
Departamento de Física
Universidad de Extremadura
06071, Badajoz (Spain)
Dr. D. K. Kim
Department of Materials Science and Engineering
Korea Advanced Institute of Science and Technology
Yusong, Taejon 305-701 (Korea)
Dr. S. Wuttiphan
National Metal and Materials Technology Center
Bangkok 10400 (Thailand)
Dr. I. M. Peterson
Corning Inc.
Corning, NY 14831 (USA)
Dr. X. Hu
Department of Mechanical and Materials Engineering
The University of Western Australia
Nedlands, WA 6907 (Australia)

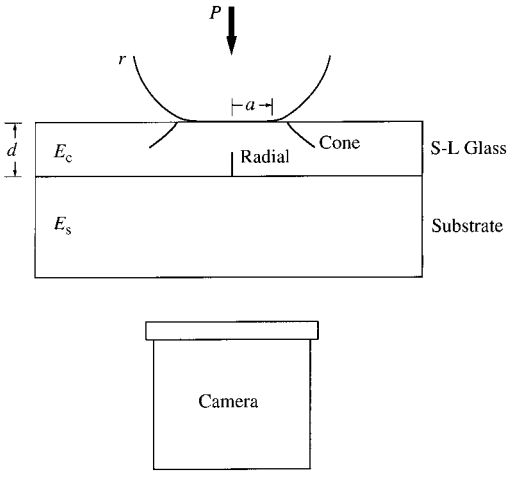

Fig. 1. Schematic of brittle coating on a compliant substrate, depicting sphere indenter and resultant surface-initiated cone and subsurface-initiated radial cracks.

$$P_{cone} = AG_c r \quad (1)$$

where A is a dimensionless constant and G_c is the crack resistance (toughness). Equation 1 is the well-documented "Auerbach's law".[16,17] Notwithstanding the fact that the crack must start from a surface flaw, P_{cone} is insensitive to initial flaw size. Thus, it is toughness G_c and not strength that governs in this case. Equation 1 is independent of thickness d, because crack initiation occurs in the near-contact field.

Radial cracks: This is a relatively new fracture mode, unique to layer structures in concentrated loads.[9,10,12,18] The cracks pop in at the bottom surface of the coating (i.e., at the coating/substrate interface) immediately below the contact, and extend radially over large lateral distances as the load is increased beyond the critical value. They remain subsurface during this lateral extension and so are not easily detected in opaque coatings. The tensile stress component responsible for this insidious form of damage is from flexure of the coating, and so has a dependence $\sigma \propto P/d^2$ characteristic of plates in bending.[19] Radial cracking initiates spontaneously from a starting surface flaw at a critical load P_{rad}, when σ equals the bulk flexure strength σ_F of the coating.[15] Resort to an engineering stress analysis for an infinitely wide center-point-loaded slab (coating) on a compliant foundation (substrate)[19] yields the explicit relation

$$P_{rad} = B\sigma_F d^2/\log(CE_c/E_s) \quad (2)$$

in the limit of small contact radius ($a \ll d$, Fig. 1) and coating surface displacement, with E_c and E_s respective Young's moduli and B and C dimensionless constants. Equation 2 represents an entirely new formulation in the context of brittle coatings. The quantity C is expected to be close to unity, because the flexure component of the stress field must vanish in monoliths ($P_{rad} \to \infty$, $E_c = E_s$). It is strength σ_F that now governs. Note that P_{rad} is insensitive to sphere radius r, reflective of a far-field solution.

We illustrate with data for first cracking induced by a WC sphere of radius r = 3.96 mm on soda-lime glass (modulus E_c = 70 GPa) plates of thicknesses d = 100 μm to 6 mm, bonded with a thin layer (<10 μm) of epoxy adhesive onto thick (12.5 mm), transparent low-modulus glass (E_s = 44 GPa and 20 GPa) and polycarbonate plastic (E_s = 2.35 GPa) substrates. The interlayer adhesion is sufficiently strong that delamination is never observed in our experiments. Both upper and lower surfaces of the soda-lime glass coatings are abraded with 600 SiC grit prior to bonding to the substrates to ensure homogeneity of flaw sizes and densities for crack initiation. A singular advantage of transparent layers is that one may observe and measure critical loads for crack initiation in situ using a camera below the contact, Figure 1. Examples of each kind of crack are shown in Figure 2. Critical load data are plotted in Figure 3 as a function of d, for each modulus E_s relative to E_c. Solid lines through the data correspond to fitted parameters in Equations 1 and 2: for cone cracks, $A = 7.4 \times 10^3$, using G_c = 7.7 J m^{-2} for soda-lime glass;[20] for radial cracks, B = 2.04 and C = 0.94, using σ_F = 110 MPa for abraded soda-lime glass.[15] Whereas cone cracking is not sensitive to d or E_c/E_s, radial cracking most certainly is, consistent with ex-

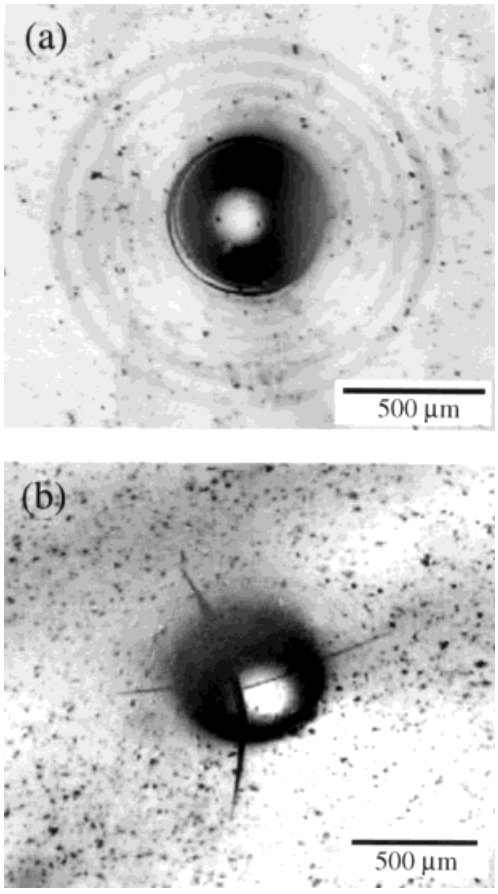

Fig. 2. Micrographs of cracks produced in soda-lime glass coating (E_c = 70 GPa) on lower modulus glass substrate (E_s = 44 GPa) from contact with WC sphere, r = 3.96 mm: a) cone crack, coating thickness d = 820 μm, load P = 375 N; b) radial crack, coating thickness d = 400 μm, load P = 250 N. Controlled surface abrasions on the coating surfaces are visible.

ADVANCED ENGINEERING MATERIALS

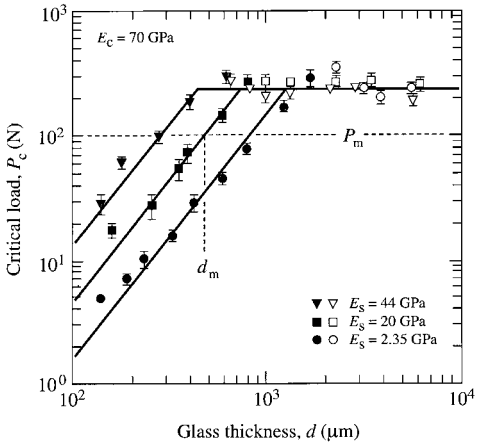

Fig. 3. Critical fracture loads for layer structures of soda-lime glass plates (E_c = 70 GPa) on soft glass and polycarbonate substrates (E_s indicated). Unfilled symbols denote cone cracks, filled symbols denote radial cracks. Solid curves are fits to Equations 1 and 2. Dashed horizontal line indicates design load P_m; corresponding coating thickness d_m indicated for E_s = 20 GPa.

pectation from Equations 1 and 2. The strong decline of P_{rad} with diminishing d on compliant substrates signals a particularly dangerous mode of fracture.

Equations 1 and 2 provide a simple basis for designing against first fracture in brittle coating structures subjected to concentrated loads. It is necessary to remain in the "safe" region beneath the solid lines in Figure 3. Suppose that an application specifies a maximum tolerable load P_m. This load corresponds to critical dimensions r_m and d_m in Equations 1 and 2: for P_m = 100 N say, we calculate $r_m \approx 1.8$ mm, $d_m \approx 0.5$ mm at E_s = 20 GPa. The first requirement for crack-free brittle coatings is simply to ensure that the effective radius of the contacting body always exceeds r_m (avoid sharp contacts). The second, more stringent requirement is to maintain the coating thickness greater than d_m (avoid thin layers), which in turn places some restriction on the lower limit of modulus E_s relative to E_c (avoid very compliant substrates). This second requirement runs counter to those of the crack-containment philosophy outlined earlier, so that optimum design may demand compromises if some damage tolerance is to be retained—e.g., remain to the right, but not too far to the right, of d_m in Figure 3. In the context of dental structures,[1] it is pertinent to recall that P_m = 100 N is a high-end biting force in oral function; that the modulus of tooth enamel and restorative porcelain veneer is E_c = 65–70 GPa (similar to our soda-lime glass coating) relative to E_s = 15–20 GPa for dentin (similar to our intermediate substrate modulus); that typical cuspal radii lie within r = 2 to 4 mm (slightly higher than our estimate of r_m); and that tooth and crown structures lie within a thickness range d = 1–2 mm (comfortably higher than our estimate of d_m). We are currently using these principles, in close collaboration with dental clinicians, to design more damage-resistant, longer-lifetime crowns.

The above formulation identifies toughness G_c and strength σ_F as important coating fracture parameters. In glasses and fine-grain polycrystalline ceramics with single-valued toughness (implicit in our derivations), increasing one of these parameters usually increases the other (as well as elastic modulus). On the other hand, in heterogeneous, coarse-grain ceramics with weak internal (grain boundary) interfaces, strength and toughness tend to be inversely related.[21] The weak interfaces deflect the cracks and cause interlocking grains to "bridge" opposite walls behind the advancing tip, progressively increasing the toughness as the crack extends ("crack-resistance curve").[22] Conversely, these same microstructural-scale weaknesses tend to diminish the toughness in the short-crack domain of natural flaws, degrading the strength. They also promote an alternative form of cumulative microdamage beneath the contact, which can lead to greatly accelerated fatigue and wear.[23] Hence, contrary to conventional expectation, high "toughness" does not guarantee improved performance, and may in fact degrade it. High strength is the more important coating fracture property. We note that, given the above evaluations of B and C, Equation 2 may be transposed to enable useful estimates of strengths of brittle coatings from simple measurements of critical loads to radial fracture.

The strength requirement means that one needs to avoid large surface flaws in the brittle coating, either natural or inadvertent (e.g., by machining), since σ_F varies with the inverse square root of flaw size.[17,24] Thus P_{rad} in Equation 2 also varies with the inverse square root of flaw size (although P_{cone} in Equation 1 remains relatively insensitive). Our deliberate use of abraded surfaces for experimental control means that the $P_{rad}(d)$ data in Figure 3 may be regarded as conservative estimates of practical load-bearing capacity of glassy coatings, realistically expanding the domain of safe operation to somewhat smaller thicknesses.

Equations 1 and 2 appeal because of their simple closed form. They are not exact: the coefficient A in Equation 1 may depend slightly on d (Fig. 3), as well as on Poisson's ratio of the coating material and modulus of the indenter;[25] the coefficient B in Equation 2 also depends slightly on d, especially in the region of very thin films,[15] and C slightly on the ratio a/d (Fig. 1).[19] Of course, any practical application of Equations 1 and 2 should always be augmented with experimental data on real systems, or numerical analysis using finite element algorithms. Nevertheless, we believe that our formulation provides a sound physical basis for designing brittle coating structures against lifetime-threatening damage in exacting concentrated loading conditions.

Received: August 15, 2000

[1] I. M. Peterson, A. Pajares, B. R. Lawn, V. P. Thompson, E. D. Rekow, *J. Dental Res.* **1998**, *77*, 589.
[2] W. J. Clegg, *Science* **1999**, *286*, 1097.
[3] J. Cook, J. E. Gordon, *Proc. R. Soc. London A* **1964**, *282*, 508.
[4] W. J. Clegg, K. Kendall, N. M. Alford, T. W. Button, J. D. Birchall, *Nature* **1991**, *347*, 455.
[5] R. Lakshminarayanan, D. K. Shetty, R. A. Cutler, *J. Am. Ceram. Soc.* **1996**, *79*, 79.
[6] M. P. Rao, A. J. Sánchez-Herencia, G. E. Beltz, R. M. McMeeking, F. F. Lange, *Science* **1999**, *286*, 102.

[7] D. B. Marshall, *Am. Ceram. Soc. Bull.* **1992**, *71*, 969.
[8] M. C. Shaw, D. B. Marshall, M. S. Dadkhah, A. G. Evans, *Acta Metall.* **1993**, *41*, 3311.
[9] S. Wuttiphan, B. R. Lawn, N. P. Padture, *J. Am. Ceram. Soc.* **1996**, *79*, 634.
[10] L. An, H. M. Chan, N. P. Padture, B. R. Lawn, *J. Mater. Res.* **1996**, *11*, 204.
[11] H. M. Chan, *Annu. Rev. Mater. Sci.* **1997**, *27*, 249.
[12] H. Liu, B. R. Lawn, S. M. Hsu, *J. Am. Ceram. Soc.* **1996**, *79*, 1009.
[13] N. P. Padture, B. R. Lawn, *J. Am. Ceram. Soc.* **1995**, *78*, 1431.
[14] D. K. Kim, Y.-G. Jung, I. M. Peterson, B. R. Lawn, *Acta Mater.* **1999**, *47*, 4711.
[15] H. Chai, B. R. Lawn, S. Wuttiphan, *J. Mater. Res.* **1999**, *14*, 3805.
[16] F. C. Frank, B. R. Lawn, *Proc. R. Soc. London A* **1967**, *299*, 291.
[17] B. R. Lawn, *Fracture of Brittle Solids*, 2nd ed., Cambridge University Press, Cambridge **1993**, Ch. 8.
[18] T. J. Lardner, J. E. Ritter, G.-Q. Zhu, *J. Am. Ceram. Soc.* **1997**, *80*, 1851.
[19] S. Timoshenko, S. Woinowsky-Krieger, *Theory of Plates and Shells*, 2nd ed., McGraw-Hill, New York **1959**, Ch. 8.
[20] S. M. Wiederhorn, *J. Am. Ceram. Soc.* **1969**, *52*, 99.
[21] L. M. Braun, S. J. Bennison, B. R. Lawn, *J. Am. Ceram. Soc.* **1992**, *75*, 3049.
[22] P. L. Swanson, C. J. Fairbanks, B. R. Lawn, Y.-W. Mai, B. J. Hockey, *J. Am. Ceram. Soc.* **1987**, *70*, 279.
[23] F. Guiberteau, N. P. Padture, H. Cai, B. R. Lawn, *Philos. Mag. A* **1993**, *68*, 1003.
[24] A. A. Griffith, *Philos. Trans. R. Soc. London A* **1920**, *221*, 163.
[25] B. R. Lawn, *J. Am. Ceram. Soc.* **1998**, *81*, 1977.

Image Analysis of Millistructure for Mechanical Characterization of Aluminum Foam

By *Marco Valente*,* *Marco Parisi*, and *Francesca Nanni*

During the past few years there has been increasing interest in the study and production of metallic foams.[1] These materials have a very high stiffness-to-weight ratio and interesting thermostructural characteristics that, since they depend on the relative density, are adjustable to multifarious needs. Metallic foams are cellular materials that can bear heavy loads, achieving an excellent compromise of stiffness, strength, and weight. Thus these materials can be employed not only as fillers, but also for particular structural functions. It is easy to understand why there is great interest in the industrial uses of these materials. In fact, foams are potentially the best materials for a great number of industrial applications, even if their production and characterization present some difficulties.

Metallic foams are a relatively recent development and, therefore, knowledge of their mechanical properties is not exhaustive. Mathematical models for the behavior of metallic foams are not optimized and it is sometimes necessary to borrow models from polymer foam science,[2] though this does not always give accurate results.

The aim of our work was to optimize a mathematical equation for predicting the plateau stress (the part of the curve just after the elastic limit) of aluminum foams of different densities. The foam we studied is made by Alcan by a metallurgical melting route. We determined numerically the correct equation and verified it with static compression tests and observations with the optical microscope. The two kinds of test were carried out on several specimens of two different densities (0.16 and 0.32 g/cm^3). In order to achieve our objective, the work was split into two phases: first the formulation of the equation (before which, however, it was necessary to undertake preliminary compression tests), and second the validation of the model. Our results show the appropriateness of the model and a good match between the experimental and calculated plateau stress values.

From various plateau stress evaluation models for cellular materials in the scientific literature,[2–4] we chose the following to represent our aluminum foam.

$$\frac{\sigma^*_{pl}}{\sigma_y} = C_4\left(\Phi\cdot\frac{\rho^*}{\rho_s}\right)^{\frac{3}{2}} + C_5(1-\Phi)\left(\frac{\rho^*}{\rho_s}\right) \quad (1)$$

Here σ^*_{pl} is the plateau stress, σ_y is the yield stress of the monolithic material, ρ^* is the foam density expressed in g/cm^3, ρ_s is the density of the monolithic material, $(1-\Phi)$ is the volume solid fraction present in the wall cells, while Φ is the solid volume fraction present in the edges and estimated by the following expression.

$$\Phi = \frac{t_e^2}{t_e^2 + \frac{Z_f}{\bar{n}} t_f l} \quad (2)$$

In Equation 2, t_f is the face thickness, t_e the edge thickness, n is the average number of edges for each wall of the single cell, l is the average length of the walls, and Z_f is the number of walls in each edge. All the variables present in Equation 2 have been derived by image analysis. In Figure 1b it is possible to see, as an example, one of the images from which these variables have been calculated.

[*] *Prof. M. Valente, Dr. M. Parisi, Dr. F. Nanni*
Department of Chemical and Material Engineering (ICMMPM)
University of Rome „La Sapienza"
Via Endossiana 18, 00184 Roma (Italy)
E-mail: Marco.valente@ingchim.ing.uniroma1.it